

# Thermal activated detection of dark particles in a weakly coupled quantum Ising ladder

Yunjing Gao<sup>1,\*</sup>, Jiahao Yang<sup>1,\*</sup>, Huihang Lin<sup>2,3</sup>, Rong Yu<sup>2,3</sup> and Jianda Wu<sup>1,4,5,†</sup>

<sup>1</sup>*Tsung-Dao Lee Institute, Shanghai Jiao Tong University, Shanghai 201210, China*

<sup>2</sup>*Department of Physics and Beijing Key Laboratory of Opto-electronic Functional Materials and Micro-nano Devices, Renmin University of China, Beijing 100872, China*

<sup>3</sup>*Key Laboratory of Quantum State Construction and Manipulation (Ministry of Education), Renmin University of China, Beijing, 100872, China*

<sup>4</sup>*Shanghai Branch, Hefei National Laboratory, Shanghai 201315, China*

<sup>5</sup>*School of Physics and Astronomy, Shanghai Jiao Tong University, Shanghai 200240, China*

(Dated: June 24, 2024)

The Ising<sub>h</sub><sup>2</sup> integrable field theory, which emerges when two quantum critical Ising chains are weakly coupled, possesses eight types of relativistic particles whose mass spectrum and scattering matrices are organized by the  $\mathcal{D}_8^{(1)}$  algebra. It is predicted that all odd-parity particles are dark and cannot be directly excited from the ground state. This makes these dark particles hard to be detected. Here, we study the local dynamical spin structure factor of the model at low-frequencies and low-temperatures. In contrast to the invisibility of the dark particles in THz spectroscopy or inelastic neutron scattering measurement, we find that the lightest dark particle is detectable, manifested as a thermal activation gap in nuclear magnetic resonance measurements. Our results provide a practical criterion for verifying the existence of dark particles.

*Introduction.*— Quantum criticality acts as a key framework for understanding a wide range of collective behaviors in many-body systems within the quantum critical region [1]. A notable feature of quantum criticality lies in its ability to manifest quantum field theories as low-energy effective descriptions for systems with microscopic origins. This connection is particularly evident in certain one-dimensional (1D) systems, where conformal invariance and/or integrability become apparent [2, 3], revealing underlying structures and scaling laws for excitations, dynamics, etc. A paradigmatic quantum model is the transverse field Ising chain (TFIC), whose quantum critical point (QCP) is governed by a central charge 1/2 conformal field theory [4]. Introducing Ising field perturbation into critical TFIC further leads to the emergence of quantum  $E_8$  integrable field theory, with delicate mathematical structure embedded in its spectrum [5, 6]. In recent years, these theoretical predictions have been confirmed in quasi-1D magnetic materials through combined efforts from THz spectroscopy [7, 8], nuclear magnetic resonance (NMR) [9], and inelastic neutron scattering (INS) experiments [10].

Integrable systems can also be categorized within the framework of coupled conformal field theory. Specifically, for the quantum Ising ladder composed of two weakly-coupled critical TFICs, its low-energy physics is described by the Ising<sub>h</sub><sup>2</sup> integrable field theory (IIFT). The IIFT contains eight types of relativistic particles, 6 breathers ( $B_n$ ,  $n = 1, 2 \dots 6$ ), a soliton ( $A_{+1}$ ) and an anti-soliton ( $A_{-1}$ ), whose mass spectrum and scattering matrices are exotically organized by the  $\mathcal{D}_8^{(1)}$  algebra [11]. Excitations in this model can be characterized in terms of single- and multi- particles. Among them,  $B_{1,3,5}$ , referred to “dark particles”, are posited to be inherently prohib-

ited from the ground state through any local or quasi-local spin operations, due to global selection rules. [12] Remarkably, the lightest dark particle, once prepared, is theorized to be robust and long lifetime as decay channels through local or quasi-local spin fluctuations are forbidden [12]. The absence of single dark particle peaks in the zero-temperature dynamical structure factor (DSF) is validated numerically [13]. Even though dark particles contribute to the spectra via multi-particle processes, their spectral signatures are expected to be elusive in THz spectroscopy of materials predicted to exhibit the Ising<sub>h</sub><sup>2</sup> physics [13, 14]. Given the intriguing properties and significant potential applications of dark particles, it is desired to have a proper experimental setup capable of directly confirming the presence of single dark particles.

In this letter, after introducing the dark particles in the IIFT, we analytically determine the relation between gap and interchain coupling constant. Then we analyze asymptotic behaviors of the local spin DSF in low-frequency and low-temperature limit. Our results show that the thermal activation gap extracted from the local DSF directly corresponds to the mass of the lightest dark particle  $m_{B_1}$ , instead of the lightest visible particle  $m_{B_2} \approx 1.95m_{B_1}$ . The characteristic feature can serve as a distinctive sign to confirm the existence of the lightest dark particle  $B_1$ . Accordingly, we propose that the  $B_1$  particle can be observed through proper NMR relaxation rate measurements.

*The model.*— The Hamiltonian of two weakly-coupled quantum critical transverse-field Ising chains fol-

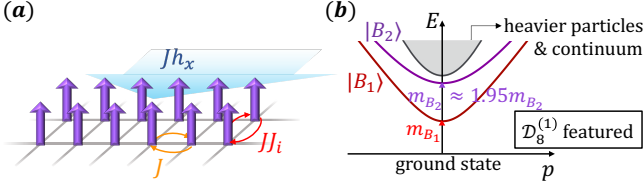


FIG. 1. (a) Illustration of two weakly coupled quantum Ising chains with transverse field  $Jh_x = J$ . (b) Energy spectrum of IIFT and mass relation between the lightest two particles.

lows

$$H = -J \sum_{l=1,2} \sum_{n=1}^{N-1} (\sigma_n^{z(l)} \sigma_{n+1}^{z(l)} + h_x \sigma_n^{x(l)}) - J \sum_{n=1}^N J_i \sigma_n^{z(1)} \sigma_n^{z(2)} \quad (1)$$

where  $\sigma_n^{\mu(1,2)}$  are Pauli matrices associated with spin operators  $S^\mu = \sigma^\mu/2$  ( $\hbar = 1, \mu = x, y, z$ ) at site  $n$  on chain (1) or (2).  $J$  and  $J_i$  are intra- and inter-chain couplings, respectively. For two decoupled TFICs, Jordan-Wigner transformation maps spins into a set of fermion operators  $c_n, c_n^\dagger$  (omit chain notations), which can be diagonalized by Bogoliubov transformation, leading to gapless dispersion for  $h_x = 1$  [15, 16]. Majorana spinors can be defined through  $\psi_{L,R}(n) = (-1)^j (e^{\pm i\pi/4} c_n + e^{\mp i\pi/4} c_n^\dagger) / \sqrt{2a}$ . In the scaling limit lattice spacing  $a \rightarrow 0$ ,  $J \rightarrow \infty$  with  $2Ja = 1$ , low-energy region of a single chain is effectively represented by the central charge  $1/2$  conformal field theory (CFT)  $H_{c=1/2}^{(l)}$ , ( $l = 1, 2$ ) [17, 18], whose Hamiltonian density  $\tilde{H}_{\text{Majorana}} = (i/2) (\psi_L \partial \psi_L / \partial x - \psi_R \partial \psi_R / \partial x)$  with continuous  $\psi_{R/L}(x)$  defined from  $x = na$ . Parallely, scaling limit of  $\sigma_j^z$  and  $\sigma_j^x$  can be taken, conventionally referred to as order operator  $\sigma(x)$  and energy operator  $\epsilon(x)$ , keeping their relations with the spinors.

In the presence of weak interchain coupling, the perturbed Hamiltonian follows

$$H = H_{c=1/2}^{(1)} + H_{c=1/2}^{(2)} + \gamma \int dx \sigma^{(1)}(x) \sigma^{(2)}(x). \quad (2)$$

It is convenient to combine the aforementioned two sets of Majorana fermions into Dirac fermions, i.e.,  $\chi_{L,R} = (\psi_{L,R}^{(1)} + i\psi_{L,R}^{(2)}) / \sqrt{2}$  [18]. Two copies of  $\tilde{H}_{\text{Majorana}}$  are grouped as  $\tilde{H}_{\text{Dirac}} = (i/2) (\chi_L^\dagger \partial \chi_L / \partial x - \chi_R^\dagger \partial \chi_R / \partial x)$  with  $\dots$  denoting the normal ordering. Then the Dirac fermions can be mapped to bosonic fields  $\phi_{L,R}$  through  $\chi_{L,R} = (\alpha_{L,R} / \sqrt{N}) : \exp(\mp \phi_{L,R}) :$ , where  $\alpha_{L,R}$  ensures the anticommutation relation of  $\chi_{L,R}$ , leading to the free boson theory  $\tilde{H}_{\text{Boson}} = (\partial \phi / \partial x)^2$ . This gives other bosonization correspondences as:  $\sigma^{(1)}(x) \sigma^{(2)}(x) \rightarrow : \cos \phi(x) / 2 :$ ,  $\epsilon^{(1)}(x) + \epsilon^{(2)}(x) \rightarrow : \cos \phi(x) :$  and  $\epsilon^{(1)}(x) - \epsilon^{(2)}(x) \rightarrow : \cos \Theta(x) :$  where the dual field  $\Theta(x)$  satisfies  $\partial \Theta(x) / \partial x = -\partial \phi(x) / \partial t$  [18].

After bosonization, the low-energy sector of Eq. (1) is

TABLE I: Parity and topological charge of the 8 single particles, ground state and  $\phi$  field [20, 21].

	$B_{1,3,5}$	$B_{2,4,6}$	$A_+$	$A_-$	$ 0\rangle$	$\phi$
parity	odd	even	/	/	even	odd
topological charge	0	0	+1	-1	0	/

captured by the IIFT [11]

$$H_{\text{IIFT}} = \int dx \left[ \frac{1}{2} \left( \frac{\partial \phi}{\partial t} \right)^2 + \frac{1}{2} \left( \frac{\partial \phi}{\partial x} \right)^2 + \lambda \cos \frac{\phi(x)}{2} \right] \quad (3)$$

defined on a  $\mathbb{Z}_2$  orbifold, with rescaled interchain coupling  $\lambda = \sqrt{2}\gamma$  [19]. The theory accommodates 8 types of particles with masses  $m_{B_n} = m_{B_1} \sin(n\pi/14) / \sin(\pi/14)$  ( $n = 1, 2, \dots, 6$ ) and  $m_{A_\pm} = m_{B_1} / (2 \sin(\pi/14))$ , whose scattering matrices and mass spectrum can be organized by the  $\mathcal{D}_8^{(1)}$  Lie algebra [11]. These single particles together with their combinations form a complete basis, each described by  $|P_1(\theta_1)P_2(\theta_2)\dots\rangle$  with particle type  $P$ , rapidity  $\theta$ , eigenenergy  $E_{\{r\}} = \sum_{j=1}^r m_{P_j} \cosh \theta_j$  and eigenmomentum  $p_{\{r\}} = \sum_{j=1}^r m_{P_j} \sinh \theta_j$  [3]. As demonstrated in Ref. [12], transition between even- and odd-parity states via any local or quasi-local spin operations is forbidden. In particular, the lightest particle  $B_1$  (with parity odd) cannot be excited from nor decay to the ground state since it is parity even [Tab. I].

*Scaling for  $m_{B_1}$ .* — Following similar strategy in [22], we fix the normalization condition for coupling constant in the lattice model [Eq. (1)] and its scaling limit [Eq. (2)] by

$$\left\langle \gamma \int dx \sigma^{(1)}(x) \sigma^{(2)}(x) \right\rangle = \left\langle J \sum_{n=1}^N J_i \sigma_n^{z(1)} \sigma_n^{z(2)} \right\rangle, \quad (4)$$

which is recovered as  $\gamma L \langle \sigma^{(1,2)} \rangle^2 = J J_i N \langle \sigma^{z(1,2)} \rangle$  in the decoupled limit. Consider  $h_x \rightarrow 1^-$ , then the magnetization in lattice and continuum limit follow by  $\langle \sigma \rangle = 2^{1/12} e^{-1/8} \mathcal{A}^{3/2} \Delta^{1/8}$  and  $\langle \sigma^z \rangle = (1 - h_x^2)^{1/8}$ , respectively,

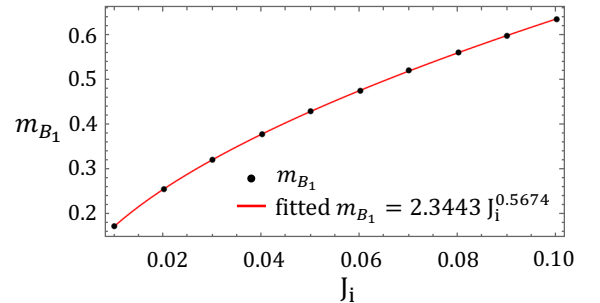


FIG. 2. Relation between  $m_{B_1}$  and  $J_i$ . The black dots are calculated from DMRG method with  $N = 400$  for each chain and  $J = 1$ . The fitted relation between  $m_{B_1}$  and  $J_i$  is shown in red line, which agrees well with analytical result  $m_{B_1} = 2.3797 J_i^{4/7}$  from Eq. (6).

where the gap  $\Delta = 2J(1 - h_x)$  and the Glaisher's constant  $\mathcal{A} = 1.282427\dots$  [23]. As a result,

$$\gamma = \frac{2J_i J^{7/4}}{(2^{1/12} e^{-1/8} \mathcal{A}^{3/2})^2}. \quad (5)$$

The  $m_{B_1}$  in the IIFT follows  $m_{B_1} = (\lambda/\mathcal{C}_1)^{4/7}$  with  $\mathcal{C}_1 = 0.33645\dots$  [19]. Combining with  $\lambda = \sqrt{2}\gamma$  and Eq. (5), we arrive at

$$m_{B_1} = \left( \frac{2\sqrt{2}}{\mathcal{C}_1 2^{1/6} e^{-1/4} \mathcal{A}^3} \right)^{4/7} J_i^{4/7} J. \quad (6)$$

Coefficients determined here are consistent with numerical calculation [Fig. 2], where  $m_{B_1}$  is obtained from the energy of the first excited state, following the density matrix renormalization group (DMRG) method [24, 25].

*Spin dynamics.*— Local spin DSF at finite temperature follows

$$C^\mathcal{O}(\omega, T) = \int_{-\infty}^{\infty} dt e^{i\omega t} \langle \mathcal{O}(t, 0) \mathcal{O}^\dagger(0, 0) \rangle_T, \quad (7)$$

where  $\mathcal{O}$  denotes the field theory counterpart of local spin operators. Using field theory language, the DSF can be expressed in the Lehmann spectral representation as,

$$C^\mathcal{O}(\omega, T) = \frac{1}{\mathcal{Z}} \sum_{i,f} C_{i,f}^\mathcal{O}(\omega, T), \quad (8)$$

with  $C_{i,f}^\mathcal{O}$  labelling the contribution of excitation from  $\#i$ -particle states to  $\#f$ -particle states and the partition function  $\mathcal{Z} = \text{Tr} e^{-H/T} = \sum_{n=0}^{\infty} \mathcal{Z}_n$ . Explicitly,

$$C_{i,f}^\mathcal{O}(\omega, T) = \sum_{\mathbf{i}, \mathbf{f}} \int \frac{d\theta'_1 \dots d\theta'_i}{(2\pi)^i \mathcal{A}_i} \int \frac{d\theta_1 \dots d\theta_f}{(2\pi)^f \mathcal{A}_f} e^{-E_i/T} \cdot |\langle P'_1(\theta'_1) \dots P'_i(\theta'_i) | \mathcal{O} | P_1(\theta_1) \dots P_f(\theta_f) \rangle|^2 \delta(\omega + E_i - E_f), \quad (9)$$

and

$$\mathcal{Z}_n = \int_{\mathbf{n}} \frac{d\theta_1 \dots d\theta_n}{(2\pi)^n \mathcal{A}_n} e^{-\frac{E_n}{T}} \langle P_1(\theta_1) \dots P_n(\theta_n) | P_1(\theta_1) \dots P_n(\theta_n) \rangle, \quad (10)$$

where the Boltzmann constant  $k_B = 1$ ,  $\mathbf{i}$  labels asymptotic state containing  $i$  particles, and  $\mathcal{A}_i = \prod_{l \in \mathbf{i}} n_l!$  with  $n_l$  counting the particle number of type  $l$ . At low temperature  $T \ll m_{B_1}$  with the Boltzmann factor serving as a controlled parameter, a regularized linked cluster expansion can be obtained [26]

$$C^\mathcal{O}(\omega, T) = \sum_{i,f} D_{i,f}^\mathcal{O}(\omega, T), \quad (11)$$

where  $D_{0,f}^\mathcal{O} = C_{0,f}^\mathcal{O}$ ,  $D_{1,f}^\mathcal{O} = C_{1,f}^\mathcal{O} - \mathcal{Z}_1 C_{0,f-1}^\mathcal{O}$ ,  $D_{2,f}^\mathcal{O} = C_{2,f}^\mathcal{O} - \mathcal{Z}_1 C_{1,f-1}^\mathcal{O} + (\mathcal{Z}_1^2 - \mathcal{Z}_2) C_{0,f-2}^\mathcal{O} \dots$ .

We first study the transverse spin DSF  $C^x$  for finite but small energy ( $\omega \ll m_{B_1}$ ) at low temperature,

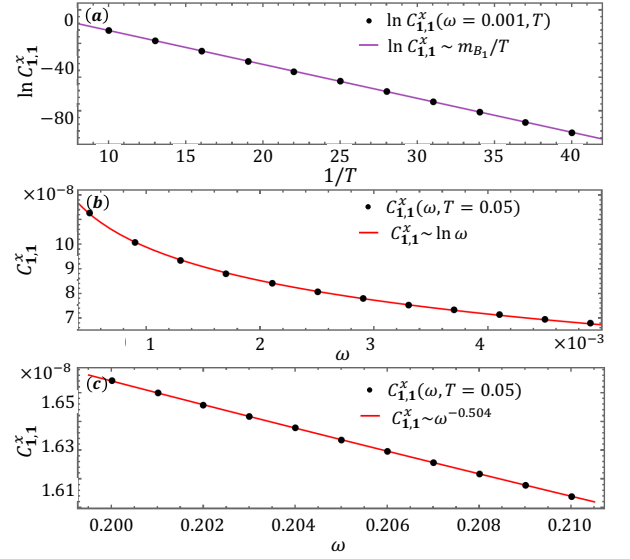


FIG. 3. Asymptotic behaviors of  $D_{1,1}^x(\omega, T)$  calculated from numerical integration of Eq. (12) with  $m_{B_1} = 1$ . (a) shows the result of fixed  $\omega$  and the fitted curve  $\log D_{1,1}^x = -1.009/T + 4.083$ . (b) and (c) show the results with fixed  $T$  in the region  $\omega \ll T$  and  $\omega \gg T$ , respectively. The curve in (b) is fitted as  $D_{1,1}^x \times 10^8 = -1.960 \log \omega + 3.647$ , and in (c)  $D_{1,1}^x \times 10^8 = 0.736 \omega^{-0.504}$ .

where  $\sigma^x$  corresponds to  $\cos \phi + \cos \Theta$  after bosonization. The operation of  $\cos \phi$  preserves topological charge while  $\cos \Theta$  connects states with topological charge-1 difference. Terms with maximum Boltzmann weight resulted from ground state excitations only contribute to the DSF after reaching  $\omega_{\text{threshold}} = m_{B_2} \approx 1.95 m_{B_1}$ , with channel  $\langle 0 | \cos \phi | B_2(0) \rangle$ , which vanishes as energy conservation can not hold for  $\omega \ll m_{B_2}$ . Then the leading term appears at the order of  $e^{-m_{B_1}/T}$  corresponding to  $|B_1\rangle \rightarrow |B_1\rangle$  channel,

$$D_{1,1}^x(\omega, T) \approx \int_{s=\pm 1} \frac{d\theta}{2\pi} \frac{e^{-m_{B_1} \frac{\cosh \theta}{T}} |\langle B_1(\theta) | \cos \phi | B_1(s\tilde{\theta}) \rangle|^2}{\sqrt{(\omega + m_{B_1} \cosh \theta)^2 - m_{B_1}^2}} e^{-m_{B_1}/T} |F_{\cos \phi}^{B_1 B_1}(i\pi)|^2 T e^{-x} \approx \int_{-\infty}^{\infty} \frac{dx}{\pi} \frac{e^{-m_{B_1}/T} |F_{\cos \phi}^{B_1 B_1}(i\pi)|^2 T e^{-x}}{\sqrt{(\omega + m_{B_1} + xT)^2 - m_{B_1}^2} \sqrt{(m_{B_1} + xT)^2 - m_{B_1}^2}} \quad (12)$$

with  $\cosh \tilde{\theta} = (\omega + m_{B_1} \cosh \theta)/m_{B_1}$ . Following form factor scheme [2],  $\langle B_1(\theta_1) | \cos \phi | B_1(\theta_2) \rangle$  depends on  $\theta_1 - \theta_2$ , obtained as  $|F_{\cos \phi}^{B_1 B_1}(i\pi)|^2 = |\langle 0 | \cos \phi | B_1(i\pi) B_1(0) \rangle|^2 = 31.756$  for  $\omega \ll m_{B_1}$  by form factor crossing relation. The second approximate sign is resulted from saddle point of the exponent in the integrand at  $\theta = 0$ . The leading behaviors of the integral in Eq. (12) can be obtained analytically [27]. For  $\omega \ll T \ll m_{B_1}$ ,

$$D_{1,1}^x(\omega, T) \approx \frac{e^{\omega/2T} |F_{\cos \phi}^{B_1 B_1}(i\pi)|^2}{\pi m_{B_1}} e^{-m_{B_1}/T} \left( -\ln \frac{\omega}{4T} - \gamma_E \right), \quad (13)$$

and for  $T \ll \omega \ll m_{B_1}$ ,

$$D_{1,1}^x(\omega, T) \approx \frac{|F_{\cos \phi}^{B_1 B_1}(i\pi)|^2}{\pi m_{B_1}} e^{-m_{B_1}/T} \left[ \sqrt{\frac{\pi T}{\omega}} - \frac{\sqrt{\pi}}{4} \left(\frac{T}{\omega}\right)^{\frac{3}{2}} \right], \quad (14)$$

In both limits,  $e^{-m_{B_1}/T}$  behavior is obtained for fixed  $\omega$  [Fig. 3 (a)], resulting in the observable thermal activation gap  $m_{B_1}$ . For the isothermal case, logarithmic divergence in  $\omega$  is found for  $\omega \ll T$  [Fig. 3 (b)] in contrast to the power law behavior for  $\omega \gg T$  [Fig. 3 (c)]. Moreover, the subleading contribution comes from the transition  $|B_2\rangle \rightarrow |B_2\rangle$ , which is negligible since the corresponding Boltzmann weight  $e^{-m_{B_2}/T} \approx e^{-1.95m_{B_1}/T} \ll e^{-m_{B_1}/T}$  for  $T \ll m_{B_1}$ .

Because the local spin along  $y$  or  $z$  direction is highly non-local in the IIFT,  $C^z$  and  $C^y$  [Eq. (11)] are beyond IIFT analytical form factor scheme. However, their thermal behaviors can be determined numerically. The first symmetry allowed channel in  $C^z$  comes from  $|B_1\rangle \rightarrow |B_1\rangle$ , dominant by zero momentum mode. Its non-vanishing spectral weight can be confirmed by calculating  $|\langle B_1(0) | \sigma^{(1,2)z}(0) | B_1(0) \rangle|^2$  in parallel to Eq. (12), effectively captured by  $W^z$  defined through

$$W^\alpha \equiv \sum_n [L \langle B_1(0) | \sigma_n^{(1,2)\alpha} | B_1(0) \rangle_L]^2 / N, \quad (15)$$

where  $\alpha = x, z$  and  $L$  denotes the lattice model.  $|B_1(0)\rangle_L$  stands for the first excited state of the lattice Hamiltonian Eq. (1). Through DMRG calculation, Fig. 4 (a) shows that both  $W^x$  and  $W^z$  converge to a finite value as the lattice size  $N \rightarrow \infty$ , suggesting non-vanishing  $C^z \sim e^{-m_{B_1}/T}$ .

The result for Ising spin is further confirmed by quantum Monte-Carlo (QMC) simulation [28], where  $C^z(\omega \rightarrow 0)$  is calculated from  $2(\pi\tau)^{-1} \sum_j \langle \delta S_i^z((2\tau)^{-1}) \delta S_i^z(0) \rangle$  with imaginary time  $\tau$  and  $\delta S_i^z = S_i^z - \langle S_i^z \rangle$  [29, 30]. The thermal activation gap fitted from Fig. 4(b) is about  $0.56J$  at  $J_i = 0.1$ , which is close to  $m_{B_1} = 0.6384J$  obtained from Eq. (6). The small deviation comes from finite temperature and finite size effect. Furthermore, the general relation for our model  $C^y = (\omega/J)^2 C^z/4$  [6, 12] implies that  $\sigma^y$  channel is negligible when  $\omega \ll J$ . Consequently, extracting the thermal activation gap from experiments enables the verification of single  $B_1$ , as elaborated in detail in the following section.

*Experimental proposal.*— In this section, we propose that the thermal activation behavior of NMR measurement can directly probe the mass of the  $B_1$  particle, confirming the existence of single  $B_1$ . For the model described in Eq. (1), the applied transverse field can serve as static magnetic field in an NMR setup [9]. The spin-lattice relaxation rate is given by [31, 32]

$$\frac{1}{T_1} \sim |A_y|^2 C^y(\omega_n) + |A_z|^2 C^z(\omega_n), \quad (16)$$

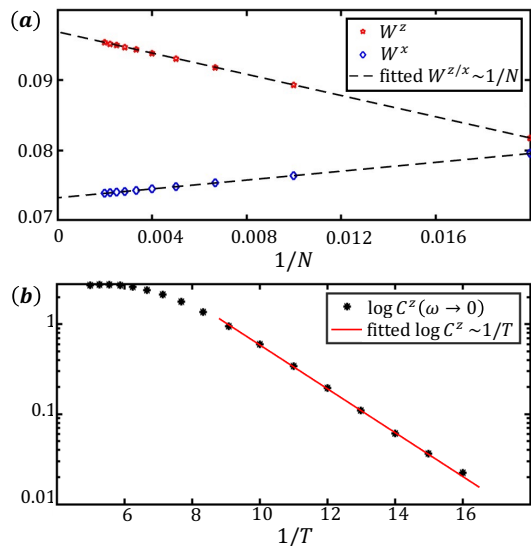


FIG. 4. (a) Relation between  $W^{z/x}$  and  $N$  obtained from DMRG calculation with  $J_i = 0.1$  and  $J = 1$ . Dashed lines show the fitting function  $W^z = -1.5172/N + 0.0969$  and  $W^x = -0.6331/N + 0.0732$ . (b) Temperature dependence of  $C^z(\omega \rightarrow 0)$  from QMC simulation with  $J_i = 0.1$ ,  $J = 1$  and  $N = 1024$ . Red line shows the fitted relation  $C^z = 160.4513e^{-0.56/T}$ .

with hyperfine coupling constant  $A_j$  ( $j = x, y, z$ ) and resonant frequency  $\omega_n$  of NMR measurement. On the other hand,  $C^x$  is related to the spin-spin relaxation rate  $1/T_2 = 1/T_1' + 1/T_2'$ , where

$$\frac{1}{T_1'} = \frac{A}{T_1}, \quad \frac{1}{T_2'} = |A_x|^2 C^x(\omega \rightarrow 0), \quad (17)$$

with constant  $A$  depending on microscopic details. Following previous discussion, the asymptotic behavior  $e^{-m_{B_1}/T}$  exhibits in all local DSFs such that  $1/T_1$  and  $1/T_2$  all behave as  $e^{-m_{B_1}/T}$ , reflecting the existence of  $B_1$  particle.

*Discussions.*— Proper Ising-chain compounds may serve as dark particle platforms. For instance, the quasi-1D magnet  $\text{CoNb}_2\text{O}_6$ , was claimed to accommodate  $E_8$  physics [14, 33], an exotic emergence after a quantum critical Ising chain is perturbed by a longitudinal field along Ising spin direction [5]. In the setup, the transverse field is tuned to the putative 1D TFIC QCP in the 3D ordering dome at low temperature ( $T \ll T_N$ ), where the 3D order is considered to effectively provide the longitudinal field coupled to the transverse-field Ising chain in the material. Recent careful analysis [13] shows that the physics is more comprehensively described by a quantum Ising ladder with  $\text{Ising}_h^2$  physics, as the putative 1D QCP lives in the vicinity of the 3D QCP in the material, a 1D model is not sufficient for treating 3D fluctuations. On the other hand, the strong magnetic frustration in the material further suppresses the effective field from the static 3D ordering background. A proper NMR measure-



ment will not only reveal the existence of the lightest dark particle  $B_1$  in the  $\text{CoNb}_2\text{O}_6$ , but also give a smoking-gun evidence, as the  $E_8$  theory has no dark particle, to confirm the  $\mathcal{D}_8^{(1)}$  physics of the material in addition to the detailed DSF analysis [13].

As a starting point for the proposed detection, we assume that thermal equilibrium has been reached in this system. Considering that the phonon-spin coupling is typically weak, the perturbation would not change the “dark” properties. Though direct excitation from ground state to dark particles is forbidden, the transition from, e.g.,  $|A_\pm\rangle$  to  $|B_1\rangle$  is permitted and  $|A_\pm\rangle$  can be excited from ground state. In contact with thermal reservoir,  $B_1$  can be reached through a secondary process  $|0\rangle \rightarrow |A_\pm\rangle \rightarrow |B_1\rangle$ . It is worth further investigating on the detailed thermalization procedure.

Different from THz or neutron scattering measurement at low temperatures ( $T \ll m_{B_1}$ ) with dominant contribution coming from excitations of ground state, the low-energy detectability ( $\omega \ll T \ll m_{B_1}$ ) of NMR can naturally probe  $F_{\cos\phi}^{B_1B_1}$  contribution. The low-temperature THz or neutron scattering measurements [14] are carried out in much wider energy region ( $0 < \omega \lesssim 10m_{B_1}$ ), where spectra contribution from  $B_1 \rightarrow B_1$  is negligible compared with  $|0\rangle \rightarrow |B_2\rangle$  and other  $\mathcal{D}_8^{(1)}$  modes, due to the strong spectra weight suppression from  $e^{-m_{B_1}/T}$  in the equilibrium ensemble.

*Conclusions.*— To conclude, following the form factor approach and cluster expansion in the region  $\omega, T \ll m_{B_1}$ , we analytically determine the thermal activation gap for  $\sigma^x$  channel, corresponding to the mass of the lightest dark particle. The same thermal activation gap is also obtained for  $\sigma^z$  following DMRG and QMC numerical calculations, which is in contrast to the first peak obtained from zero temperature spin DSF. Taking the advantage, we propose that a proper NMR experiment can detect the lightest dark particle through the relaxation rates  $1/T_1$  and  $1/T_2$  measurements where the mass of the lightest dark particle can be extracted as thermal activation gap. Potential material candidates, such as  $\text{CoNb}_2\text{O}_6$  and compounds effectively described by the Ising ladder are suggested. Cold atom and STM experiments could also directly simulate the required Ising ladder to probe the dark particles.

## ACKNOWLEDGMENTS

The work at Shanghai Jiao Tong University is supported by the National Natural Science Foundation of China Grant No. 12274288 and the Innovation Program for Quantum Science and Technology Grant No. 2021ZD0301900. The work at Renmin University of China is supported by the National Key R&D Program of China (Grant No. 2023YFA1406500), and the Na-

tional Natural Science Foundation of China (Grant Nos. 12334008 and 12174441).

\* These authors contributed equally to the work.

† wujd@sjtu.edu.cn

- [1] S. Sachdev, *Quantum Phase Transitions*, 2nd ed. (Cambridge University Press, 2011).
- [2] F. A. Smirnov, *Form Factors in Completely Integrable Models of Quantum Field Theory* (WORLD SCIENTIFIC, 1992).
- [3] G. Mussardo, *Statistical Field Theory: An Introduction to Exactly Solved Models in Statistical Physics; 1st ed.*, Oxford graduate texts (Oxford Univ. Press, New York, NY, 2010).
- [4] A. Belavin, A. Polyakov, and A. Zamolodchikov, *Nucl. Phys. B* **241**, 333 (1984).
- [5] A. B. Zamolodchikov, *Int. J. Mod. Phys. A* **4**, 4235 (1989).
- [6] J. Wu, M. Kormos, and Q. Si, *Phys. Rev. Lett.* **113**, 247201 (2014).
- [7] Z. Wang, T. Lorenz, D. I. Gorbunov, P. T. Cong, Y. Kohama, S. Niesen, O. Breunig, J. Engelmayer, A. Herman, J. Wu, K. Kindo, J. Wosnitza, S. Zherlitsyn, and A. Loidl, *Phys. Rev. Lett.* **120**, 207205 (2018).
- [8] Z. Zhang, K. Amelin, X. Wang, H. Zou, J. Yang, U. Nagel, T. Rõ om, T. Dey, A. A. Nugroho, T. Lorenz, J. Wu, and Z. Wang, *Phys. Rev. B* **101**, 220411 (2020).
- [9] A. W. Kinross, M. Fu, T. J. Munsie, H. A. Dabkowska, G. M. Luke, S. Sachdev, and T. Imai, *Phys. Rev. X* **4**, 031008 (2014).
- [10] H. Zou, Y. Cui, X. Wang, Z. Zhang, J. Yang, G. Xu, A. Okutani, M. Hagiwara, X. Matsuda, G. Wang, G. Mussardo, K. Hódsági, M. Kormos, Z. He, S. Kimura, R. Yu, W. Yu, J. Ma, and J. Wu, *Phys. Rev. Lett.* **127**, 077201 (2021).
- [11] A. LeClair, A. Ludwig, and G. Mussardo, *Nucl. Phys. B* **512**, 523 (1998).
- [12] Y. Gao, X. Wang, N. Xi, Y. Jiang, R. Yu, and J. Wu, (2024), [arXiv:2402.11229](https://arxiv.org/abs/2402.11229).
- [13] N. Xi, X. Wang, Y. Gao, Y. Jiang, R. Yu, and J. Wu, (2024), [arXiv:2403.10785](https://arxiv.org/abs/2403.10785).
- [14] K. Amelin, J. Engelmayer, J. Viirik, U. Nagel, T. Rõ om, T. Lorenz, and Z. Wang, *Phys. Rev. B* **102**, 104431 (2020).
- [15] P. Pfeuty, *Ann. Phys.* **57**, 79 (1970).
- [16] E. Lieb, T. Schultz, and D. Mattis, *Ann. Phys.* **16**, 407 (1961).
- [17] J. B. Zuber and C. Itzykson, *Phys. Rev. D* **15**, 2875 (1977).
- [18] D. Boyanovsky, *Phys. Rev. B* **39**, 6744 (1989).
- [19] P. Baseilhac, *Nucl. Phys. B* **594**, 607 (2001).
- [20] B. Schroer and T. Truong, *Phys. Lett. B* **73**, 149 (1978).
- [21] A. O. Gogolin, A. A. Nersesian, and A. M. Tsvelik, *Bosonization and Strongly Correlated Systems* (Cambridge University Press, Cambridge, 2004).
- [22] X. Wang, M. Oshikawa, M. Kormos, and J. Wu, in preparation (2024).
- [23] B. M. McCoy and T. T. Wu, *The Two-Dimensional Ising Model* (Harvard University Press, Cambridge, MA and London, England, 1973).

- [24] U. Schollwöck, *Ann. Phys.* **326**, 96 (2011).
- [25] S. R. White, *Phys. Rev. Lett.* **69**, 2863 (1992).
- [26] B. Pozsgay and G. Takács, *J. Stat. Mech.: Theory Exp.* **2010** (11), P11012.
- [27] J. Wu, M. Kormos, and Q. Si, *Phys. Rev. Lett.* **113**, 247201 (2014).
- [28] M. E. J. Newman and G. T. Barkema, *Monte Carlo Methods in Statistical Physics* (Clarendon Press, Oxford, 1999).
- [29] Y. Fan, J. Yang, W. Yu, J. Wu, and R. Yu, *Phys. Rev. Res.* **2**, 013345 (2020).
- [30] M. Randeria, N. Trivedi, A. Moreo, and R. T. Scalettar, *Phys. Rev. Lett.* **69**, 2001 (1992).
- [31] T. Moriya, *Prog. Theor. Phys.* **28**, 371 (1962).
- [32] J. Yang, W. Yuan, T. Imai, Q. Si, J. Wu, and M. Kormos, *Phys. Rev. B* **106**, 125149 (2022).
- [33] R. Coldea, D. A. Tennant, E. M. Wheeler, E. Wawrzynska, D. Prabhakaran, M. Telling, K. Habicht, P. Smeibidl, and K. Kiefer, *Science* **327**, 177 (2010).